JOURNAL OF APPLIED ELECTROCHEMISTRY 24 (1994) 1109–1115

Effect of operating conditions on anode passivation in the electrorefining of copper

X. LING, Z. H. GU, T. Z. FAHIDY*

Department of Chemical Engineering, University of Waterloo, Waterloo, Ontario N2L 3G1, Canada

Received 2 December 1994; revised 12 April 1994

The effect of various process variables on anode passivation in copper electrorefining was investigated by combining conventional electrochemical techniques, laser-based visualization, and digital image processing in a laboratory scale copper electrorefining cell. High current density operation causes early anode passivation; in the range of 0.23 to 1.50 kA m^{-2}, the effect of current density on the onset of passivation was found to be constant. The higher the temperature the longer the time required for the onset of anode passivation. When the electrolyte is circulated, anode passivation occurs earlier than in the absence of circulation, but the effect also depends on the direction of circulation.

Nomenclature

i_a (anode) current density (kA m^{-2})
T temperature (°C)
t_p passivation time (h); (i.e., the time required for the onset of passivation)
v_d downward electrolyte circulation rate (cm^3 min^{-1})
v_u upward electrolyte circulation rate (cm^3 min^{-1})

1. Introduction

In recent years much effort has been devoted to the improvement of process efficiency and product quality of the copper electrorefining process, a major technology for more than one hundred years. High current density operation is a major challenge, since in spite of its important advantages compared to low current density operation [1, 2], a larger rate of anode slime formation, earlier anode passivation and lower cathode product quality constitute major obstacles to industrial adaptation [3]. The effect of slime formation on anode passivation has generated increasing interest in recent years, as manifested by studies of periodic phenomena during the anodic dissolution of copper [4–9]. Since slimes are an important source of noble metals, much effort has also been expended on the understanding of their structure via mineralogical characterization [10–17] and microscopic methods, supplemented with X-ray diffraction and sedimentation analysis [18, 19]. The mechanism of anode passivation has a crucial role in the understanding of the copper electrorefining process. Recently, a mathematical model for the anodic passivation of pure copper was proposed by assuming that the transport of cupric ions is the controlling step in the overall process [20, 21]. It is recognized, however, that in the case of industrial anodes with their impurities, the slime formation/detachment process can significantly influence passivation patterns [22–25].

The purpose of this paper is to summarize the results of a recent investigation on the effect of various operating conditions on the passivation of an industrial anode [22]. The mechanism of anode passivation is also discussed on the basis of visualization studies employing a laser illumination technique [26–28]. The experimental results are compared with previously published data [29–32], and a quantitative relationship between passivation time and slime formation/detachment is presented along with a qualitative discussion of mass transport during the electrolysis.

2. Experimental details

Figure 1 illustrates the experimental apparatus. The electrolytic cell was made of PVC, (except for the frontal face made of glass for video-observation) with dimensions of 4 cm × 5 cm × 12 cm, an active volume of 179 cm^3, and a 4.8 cm anode/cathode separation distance. The composition of the anode, cut from an industrial sample, is given in Table 1. The cathode was a flat piece of stainless steel, with a surface dimension of 3.3 cm × 12 cm, (active cathode area of 39.6 cm^2, only one side active). The copper anode had the dimensions of 3.3 cm × 0.6 cm × 9.7 cm and an active surface area of 20 cm^2. Prior to each experiment, the anode was polished with emery paper (grit size 600), and both electrodes were washed with Contrad-70 cleaning solution, tap water and deionized water. The electrolyte was a solution obtained by dissolving 140 g $CuSO_4 . 5H_2O$ in 140 g of aqueous sulphuric acid to yield a one-litre solution. To simplify the passivation process, no surfactant or additive was added to the electrolyte. Otherwise the operating conditions were similar to industrial practice (electrolyte temperature: 45–65 °C;

* Author to whom all correspondence should be addressed.

0021-891X

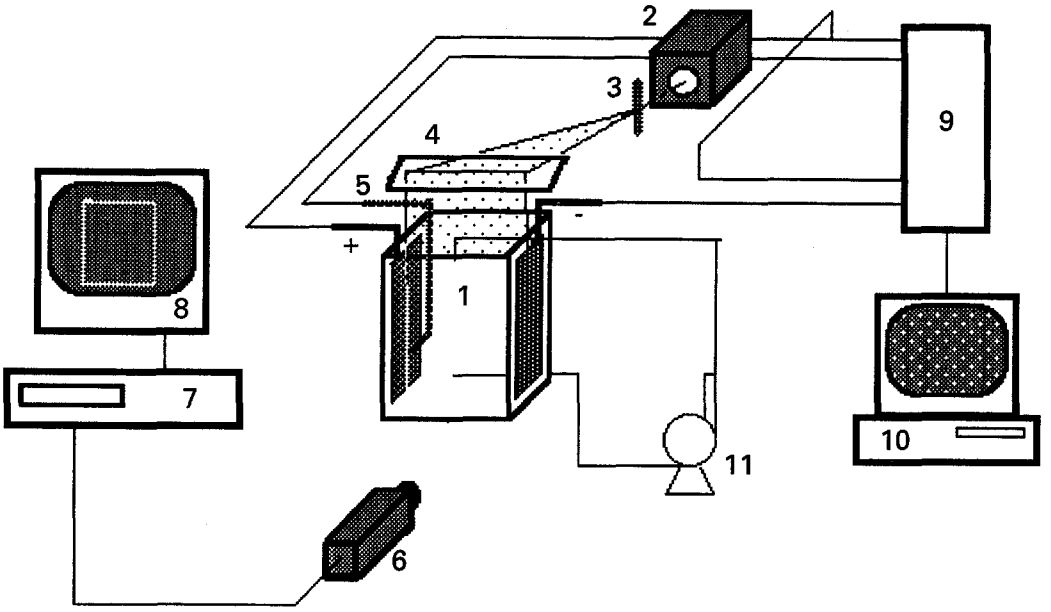

Fig. 1. Experimental apparatus: (1) cell; (2) laser, (3) glass rod, (4) mirror, (5) reference electrode, (6) video camera, (7) VCR, (8) TV monitor, (9) interface, (10) microcomputer, (11) electrolyte-circulating pump.

electrolyte flow rate: 0.93 and 1.55 $cm^3\ min^{-1}$ yielding a mean residence time of 3–5 h), excepting the current density (0.25–1.5 $kA\ m^{-2}$). The electrolyte temperature was maintained by a water bath heated with an immersed heating coil within a 1 °C range. The cell was provided with two flowports at the bottom and at the top, to allow electrolyte circulation by setting the (external) circulating pump to generate upward or downward flow in the cell. The length of an experiment was determined by the current density: at 0.25 $kA\ m^{-2}$ (common in industrial practice) anode passivation was not observed up to about 70 h. As the current density was increased, progressively lower induction periods for passivation were observed. The maximum range of passivation time reproducibility was 4.22 min. Continuous capture of images of the process was carried out by the video camera, projected on the monitor screen, and recorded on a video tape by the VCR. Slime formation and detachment of the anode surface were detected by video-monitoring. The cell potential was recorded as a time-series and stored in an IBM XT microcomputer through an OPTO-22 interface. An IBM PS/2 model 80 microcomputer equipped with a DT 2879 digital board was employed for image digitization.

3. Results and discussion

3.1. *Slime formation/detachment and anode passivation*

During electrolysis, a dark-coloured slime film appears on the initially bright anode surface, which decreases the active electrode area. As electrolysis continues, more slime is generated, the slime film becomes increasingly thicker, and the cell potential increases slightly. As seen in Fig. 2, a typical variation of cell potential with time can be divided into two sections. In the first section the potential increases monotonically, with a slight slope of about 0.16 $V\ h^{-1}$. When a sufficient amount of slime has accumulated on the anode surface, a sudden jump in the cell potential indicates the onset of oscillation (in Fig. 2, at approximately 2.4 h). At the resulting high cell potential the secondary anode reaction

$$2H_2O = O_2 + 4H^+ + 4e^- \qquad E^0 = 1.229\ V$$

becomes prominent and the large amount of oxygen bubbles generated at the anode dislodges the slime film from the electrode surface. The metal surface becomes temporarily bright after slime film detachment, but successive slime formation again produces a slime film on the metal surface. The passivation/surface reactivation cycle continues at different sites of the electrode, as shown in Fig. 3. The interaction effect with anode passivation arises from the partial reduction of the active anode surface due to the formation of the slime layer, resulting in a large surface resistance, hence larger cell potential. Individual electrode potential measurements indicate that the cathode potential remains essentially constant, hence the variation of anode potential is qualitatively similar to cell potential variations. Comparison of the phenomena recorded by the video assembly to the cell potential data, demonstrates clearly that the time instant of slime detachment from the anode surface coincides with the time instant at which the cell potential drops suddenly (at 3.2, 4.5, 5.3 h etc. in Fig. 2). An accurate quantitative estimation of the active electrode area from the images is rather difficult, however, since 'free' slime does not always begin to sink in the electrolyte upon detachment immediately, and it adheres (loosely) to the anode over a certain time period.

Table 1. Anode composition (impurity concentrations in ppm, copper in mass %); courtesy of Noranda Technology Centre, Pointe Claire, Quebec

As	*Sb*	*Bi*	*Ni*	*Se*	*Pb*	*Ag*	*Au*	*Cu*
939	312	166	2403	738	77	1956	150	>99.5

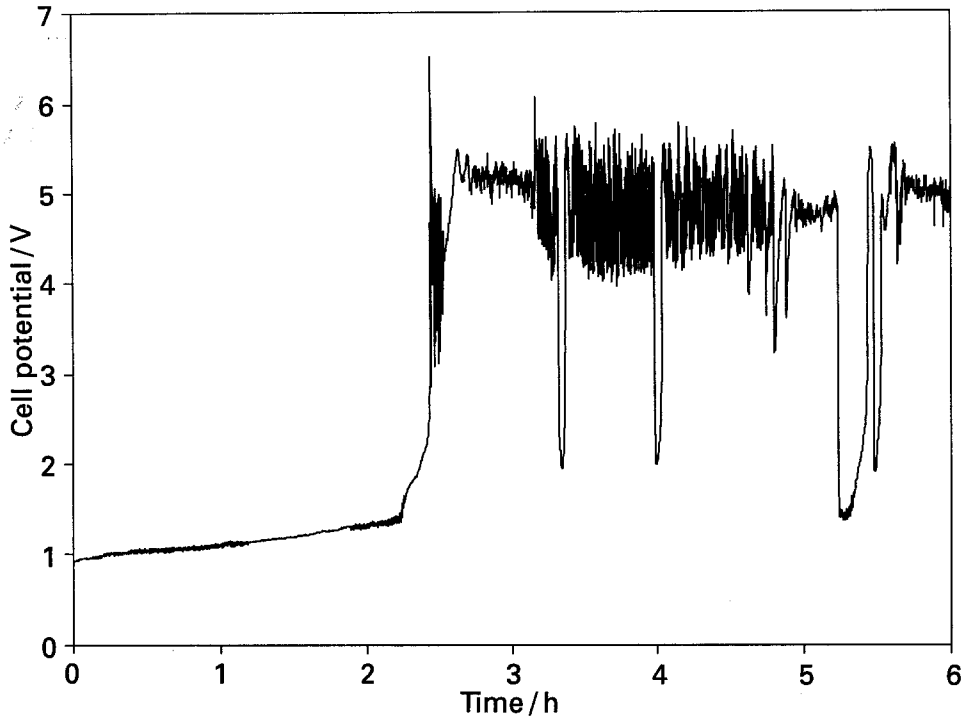

Fig. 2. The variation of cell potential with time under the conditions of $T = 55\,°C$, $i_a = 1.25\,kA\,m^{-2}$, no electrolyte circulation. The reference electrode, Hg/Hg_2SO_4/sat. aq. K_2SO_4, has a potential of 640 mV vs SHE.

3.2. *Effect of various operating conditions on anode passivation*

3.2.1. Current density. In Fig. 4, the effect of current density on passivation time is compared to earlier experimental observations reported in the literature [29–32]. The slope of the logarithmic t_p against i_a plot, valid in the 0.75–1.5 $kA\,m^{-2}$ range, compares closely to literature values ranging from −4.947 to −4.993 and is essentially insensitive to the direction

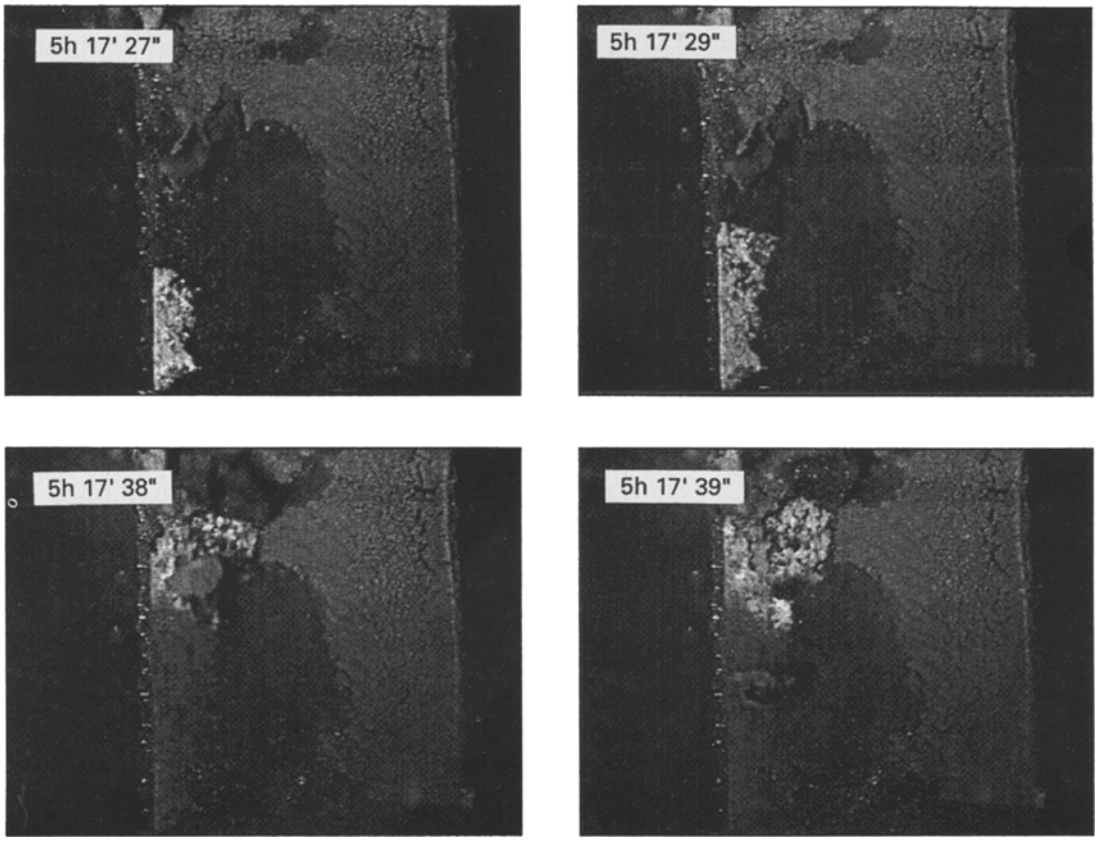

Fig. 3. Images of slime detachment from the anode surface starting at 5 h 17′ 27″ upon the onset of electrolysis, under the conditions of $T = 55\,°C$, $i_a = 1.25\,kA\,m^{-2}$, and no electrolyte circulation. At the site shown, the surface is reactivated in two seconds and the new 'fresh' area is larger. Then the fresh area is covered by new slime and reactivation continues at a different site. Some oxygen bubbles can also be seen.

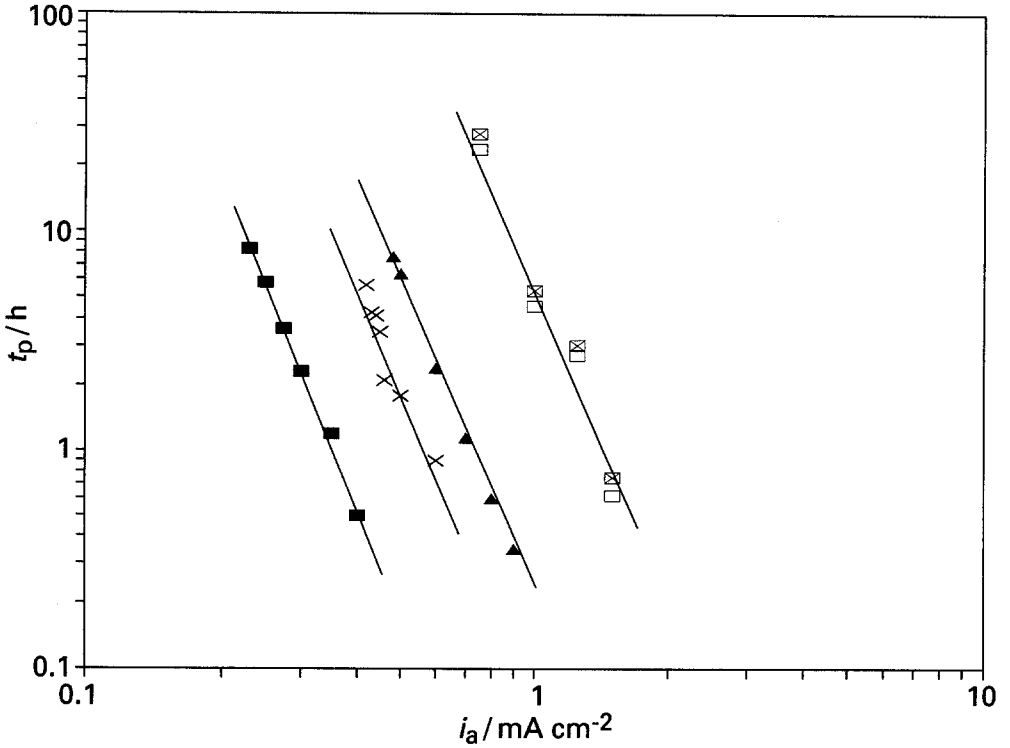

Fig. 4. The effect of current density on the onset of passivation: comparison with literature data (see Table 2). Each point shown represents an average of 2–6 experiments. In the quoted references i_a ranges from 0.23 to 1.50 kA m^{-2}. Code in Table 2: a (■), b (×), c (▲), d (⊠), e (□).

of circulation (Tables 2 and 3). This close agreement is all the more intriguing inasmuch as the electrolyte compositions, temperature and circulation rate are not identical with those employed in this work. By contrast, the intercept depends strongly on electrolyte concentration and temperature, and mildly on the direction of circulation. The exact nature of the inverse (t_p/i_a) relationship is not understood at present, but it is entirely logical to expect that an increase in the current density leads to faster anode passivation, by increasing the rate of copper dissolution and slime formation.

3.2.2. Temperature. Temperature has a beneficial effect on the copper dissolution process, as shown in Table 4: the higher the temperature, the longer the time required for the onset of passivation. The effect cannot be explained by a single phenomenon, however. On the one hand, the lower the temperature, the smaller the solubility of the slime in the electrolyte, therefore, the faster the slime accumulation on the anode surface, and earlier passivation would be expected. On the other hand, the lower the temperature, the lower the rate of copper dissolution, thus less slime (consisting mostly of Cu_2O) is generated on the anode surface in unit time, leading to retarded passivation. The overall effect, that a lower electrolyte temperature causes earlier passivation indicates the dominance of the first phenomenon.

3.2.3. Electrolyte circulation rate and circulation pattern. The effect on anode passivation is complex because rate and pattern exert not only a separate influence, but also an effect due to their mutual interaction. As demonstrated in Figs 5 and 6, anode passivation occurs earlier with circulation than without circulation, regardless of the direction of circulating flow. In upward circulation, anode passivation occurs somewhat later at higher flow rates than at lower flow rates. In downward circulation, anode passivation occurs earlier at higher flow rates than at lower flow rates. The effect of circulating flow is multifold: (i) It accelerates the

Table 2. Experimental conditions pertaining to the $\log_{10} t_P = \log_{10} k + n \log_{10} i_a$ regression lines shown in Fig. 4

*Code** (*Fig. 4*)	*Electrolyte temperature*/°C	*Flow rate*/cm^3 min^{-1} (*and direction*)	[Cu^{2+}] /mol dm^{-3}	[SO_4^{2-}] /mol dm^{-3}	*Regression* (n)	(k)
a	30	225 cm^3 min^{-1} (upward)	0.63	2.43	−4.947	0.00562
b	30	225 cm^3 min^{-1} (upward)	0.63	1.23	−4.998	0.0623
c	30	225 cm^3 min^{-1} (upward)	0.16	2.43	−4.993	0.201
d	55	1.55 cm^3 min^{-1} (upward)	0.56	1.99	−4.947	6.542
e	55	1.55 cm^3 min^{-1} (downward)	0.56	1.99	−4.954	5.644
f	55	1.55 cm^3 min^{-1} (upward and downward combined)	0.56	1.99	−4.950	6.081

* Regression parameters in cases a, b, and c were estimated from [32; Figs 3 and 4]; cases d, e and f were generated in this work.

Table 3. Effect of direction of electrolyte circulation on passivation time

i_a /kA m^{-2}	t_p/h Downward	Upward
0.75	23.9	28.0
1.0	4.60	5.37
1.25	2.75	3.03
1.5	0.62	0.75

$T = 55\,°C$, $v = 1.55\,cm^3\,min^{-1}$, $[Cu^{2+}] = 0.56\,mol\,dm^{-3}$, $[SO_4^{2-}] = 1.99\,mol\,dm^{-3}$

movement of copper ions away from the anode surface towards the bulk of the electrolyte, thus decreasing resistance to anodic copper dissolution; (ii) it carries more water molecules to the anode surface, with respect to no circulation, hence the rate of oxygen generation from anode is increased. On the one hand, both effects enhance slime formation on the anode surface. On the other hand, a certain portion of (freshly generated) slime is removed from the anode surface by circulating flow, thus delaying the onset of passivation, especially at sufficiently high circulation rates. The relative dominance of the latter function determines, under a set of experimental conditions, at what time instant will circulating flow be no longer able to remove a sufficient amount of the slime layer from the anode surface: this time instant denotes the onset of passivation. The experimental results suggest that upward flow is more efficient in 'sweeping' the anode surface thus delaying anode passivation, whereas downward flow is more efficient in retarding oxygen bubble movement away from electrode surface, hence accelerating passivation. The effect of circulating flow could be quite different at considerably higher flow rates, but high circulation rates have no current industrial significance.

3.3. *Mass transport aspects*

Due to the complex nature of the slime formation/passivation process, and the lack of quantitative kinetic data for its constituent elements, only a qualitative analysis of mass transport can be attempted at present. At the beginning of electrolysis the fresh anode surface is clean, and when the electrolyte circulation rate is low, transport near the anode surface is due mainly to liquid diffusion, that is, the diffusion of copper ions away from the anode surface

Table 4. The effect of temperature on passivation time

T /°C	*Approximate values of* t_p/h Downward flow	Upward flow
45	~1.9	~1.6
55	~4.6	~5.4
65	>8	>8

$i_a = 1\,kA\,m^{-2}$, $v = 1.55\,cm^3\,min^{-1}$, $[Cu^{2+}] = 0.56\,mol\,dm^{-3}$, $[SO_4^{2-}] = 1.99\,mol\,dm^{-3}$

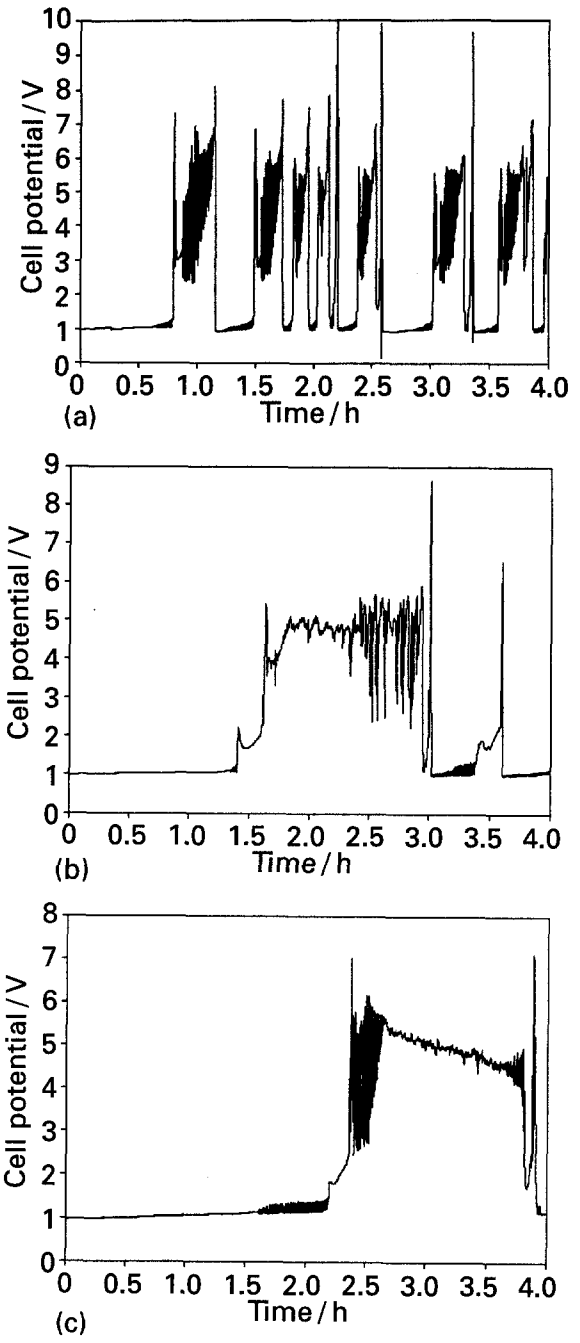

Fig. 5. The effect of upward electrolyte circulation on the onset of passivation. $i_a = 1\,kA\,m^{-2}$, $T = 45\,°C$, $v_u =$ (a) 0.93, (b) 1.55, (c) $0\,cm^3\,min^{-1}$.

into the bulk solution. The anode slime appearing during electrolysis can be considered as a porous layer. At this stage, pore diffusion, which has a higher resistance than liquid diffusion, dominates the transport and it causes a higher cell potential. The effect of liquid diffusion at this stage can be ignored. When the (sufficiently thick) slime layer begins to detach from the anode surface partially, and some of the anode surface is exposed to the electrolyte, transport at the exposed anode surface is dominated by liquid diffusion with a lower resistance. As the exposed surface is covered, once again by slime, porous diffusion will become again the controlling mode. As electrolysis progresses, the roughness of the anode surface facing the electrolyte becomes

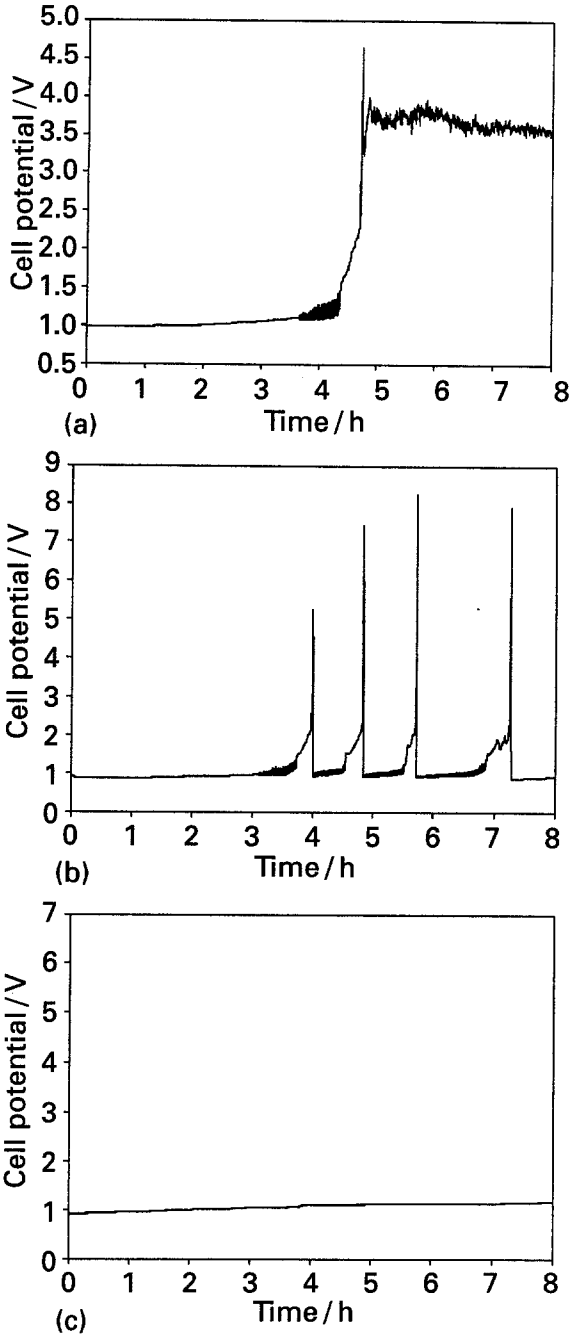

Fig. 6. The effect of downward electrolyte circulation on the onset of passivation. $i_a = 1\,kA\,m^{-2}$, $T = 55\,°C$, v_d = (a) 0.93, (b) 1.55, (c) $0\,cm^3\,min^{-1}$.

gradually larger resulting in periodic detachment of excessively long protuberances. Under such conditions, the true size of the solid/liquid interface remains unknown and mass transport coefficients cannot be calculated at reliable accuracy.

4. Conclusions

This study shows that high current density operation accelerates anode passivation. Visualization-based image processing and synchronized cell potential measurements provide a numerical relationship between passivation time and slime formation/detachment. The effect of electrolyte temperature on anode passivation is beneficial: the higher the temperature, the longer the onset period of passivation. The effects of electrolyte circulation rate and circulation pattern depend on an intricate interplay of hydrodynamic and geometric conditions. Mass transport effects are understood only qualitatively at present. The results obtained in this research should facilitate a better appreciation of certain aspects of copper electrorefining, with the usual caveats for extrapolating laboratory-size experiments to industrial cells.

Acknowledgements

This research was supproted by a strategic grant from the Natural Sciences and Engineering Research Council of Canada. Anodes donated by the Noranda Technology Centre and the INCO Roy Gordon Research Laboratory are gratefully acknowledged.

References

[1] T. Balberyszski and A. K. Andersen, TMS Extractive Metallurgy Division Symposium Proceedings, Cleveland, OH, Dec. (1968).
[2] A. K. Biswas and W. G. Davenport, *in* 'Extractive Metallurgy of Copper', Pergamon Press, Oxford (1980).
[3] G. R. Smith, F. X. McCawley, P. B. Needham and P. E. Richardson, Bureau of Mines Report of Investigation (1979), United States Department of the Interior.
[4] J. Cooper, R. M. Muller and C. Tobias, *J. Electrochem. Soc.* **127** (1980) 1733.
[5] K. Nobe, H. P. Lee and A. J. Pearlstein, *ibid.* **132** (1985) 1031.
[6] Z. H. Gu, T. Z. Fahidy and J. P. Chopart, *Electrochim. Acta* **37** (1992) 97.
[7] Z. H. Gu, J. Chen and T. Z. Fahidy, *Hydrometallurgy* in press.
[8] *Idem, Electrochim. Acta* **37** (1993) 2637.
[9] M. R. Bassett and J. L. Hudson, *Chem. Eng. Comm.* **60** (1987) 145.
[10] T. T. Chen and J. E. Dutrizac, *Can. Metall. Quart.* **27** (1988) 91.
[11] *Idem, Metallurgical Trans.* **20B** (1989) 345.
[12] *Idem, Can. Metall. Quart.* **28** (1989) 127.
[13] *Idem*, Copper '90 Refining, Fabrication, Markets, The Institute of Metals, London (1990) p. 180.
[14] *Idem, Metallurgical Trans.* **21B** (1990) 229.
[15] *Idem, Can. Metall. Quart.* **29** (1990) 293.
[16] *Idem, ibid.* **29** (1990) 27.
[17] T. T. Chen, J. E. Dutrizac and J. A. Sawiaki, Mineral Sciences Laboratories Division Report MSL 92-57(J) Draft, for publication in Nuclear Instrumental Methods for Physics Research (1992).
[18] E. N. Petkova, *Hydrometallurgy* **24** (1990) 351.
[19] Yukyo Takada, Rudi Subagja and Akio Fuwa, *J. Mining and Metallurgical Inst., Japan* **104** (1988) 289.
[20] S. Asakura, V. Baltazar and D. L. Piron, *CIM Bulletin* **79**(887) (1986) 58.
[21] D. L. Piron, S. Asakura and V. Baltazar, *CIM Bulletin* **79**(890) (1986) 82.
[22] X. Ling, M. A. Sc. thesis, Department of Chemical Engineering, University of Waterloo, Ontario, Canada (1993).
[23] A. K. Biswas and W. G. Davenport, 'Extractive Metallurgy of Copper', 2nd ed., Pergamon Press, Oxford (1980) Chapter 15.
[24] C. W. Eichrodt and J. H. Schloea, 'Copper, the Science and Technology of the Metal, its Alloys and Compounds' (edited by A. Butts), Hafnar Publishing Company, New York (1970).
[25] D. Pletcher, 'Industrial Electrochemistry', Chapman and Hall, London (1982) Chapter 4.

[26] Z. H. Gu and T. Z. Fahidy, *Int. J. Engng. Fluid Mech.* **1** (1988) 1.
[27] *Idem*, *J. Appl. Electrochem.* **19** (1989) 354.
[28] *Idem*, *Can. J. Chem. Eng.* **69** (1991) 964.
[29] J. Sedzimir and W. Gumowska, *Rudi i Metale Niezelazne* **31** (1986) 419.
[30] *Idem*, *Metalurgia i Odlewnictwo* **109** (1987) 215.
[31] *Idem*, *Arch. Metall.* **34** (1989) 17.
[32] *Idem*, *Hydrometallurgy* **24** (1990) 203.
[33] X. Ling, Z. H. Gu and T. Z. Fahidy, *Can. J. Chem. Eng.*, in press.